Experimental study of atomic 4*d* giant resonances by photoabsorption and photoelectron spectroscopy: Ba, La, and Ce

M. Richter, M. Meyer, M. Pahler, T. Prescher, E. v. Raven,
B. Sonntag, and H. E. Wetzel
II. Institut für Experimentalphysik, Universität Hamburg, Luruper Chaussee 149, D-2000 Hamburg 50, Federal Republic of Germany
(Received 14 November 1988)

Total and partial ($4d^{-1}, 4f^{-1}, 5s^{-1}, 5p^{-1}, 5d^{-1}, 6s^{-1}$) cross sections of atomic Ba, La, and Ce have been determined by absorption and photoelectron spectroscopy in the range of the giant $4d \rightarrow (4f, \epsilon f)$ resonances. Many electron theories that take polarization and relaxation effects into account describe the gross features of the spectra but in many cases fail to reproduce the exact energy positions, line shapes, and amplitudes of the resonances in the cross sections of the main and satellite lines.

I. INTRODUCTION

The large resonance structures caused by the $4d^{-1}(4,\epsilon)f$ excitations have attracted great interest in studies of photoionization of Ba and the lanthanide elements. The first absorption spectra of the lanthanide metals were obtained by Zimkina *et al.*[1] These exciting results initiated numerous detailed investigations by solid-state absorption,[2,3] photon emission,[4] and electron spectroscopy.[5–7] The interpretation in terms of atomic $4d^{-1}(4,\epsilon)f$ transitions[8–10] was corroborated by the agreement between the absorption spectra of the solids and free atoms.[3,11–16] Thanks to recent improvements in the experimental techniques[17] the difficulties encountered in photoelectron studies of free lanthanide atoms have been overcome. Electron energy distributions and partial cross sections have been reported for atomic Ba,[18,19] Ce,[20] Sm[21] and Eu.[22] Photoelectron spectroscopy is a very effective probe of the many electron dynamics and therefore well suited for stringent tests of the various theoretical approaches. The elements Ba, La, and Ce occupy key positions for the understanding of the $4d^{-1}(4,\epsilon)f$ giant resonances. In the ground state the "collapse" of the 4*f* orbital is expected to occur between Ba and La.[23–26] From spectroscopic data we know that the first 4*f* electron gets bound in Ce.[27] Excitations from Cs, Ba, and La 3*d* levels lead to 4*f* wave functions localized within the inner well of the double-well potential.[28–30] The Xe and Cs 4*d* resonances are well characterized as atomic $4d^{-1}\epsilon f$ shape resonances.[16,21,31–40] The potential barrier keeps low-energy *f* orbitals outside the core region. The $4d^{-1}\epsilon f$ maximum is centered at energies ϵ exceeding the barrier height. For 4*d* excited Ba, the inner well of the effective potential, based on a configuration-average Hartree-Fock model, is deep enough to hold a "collapsed" 4*f* orbital.[23–26,41] Term-dependent calculations show that the 4*f* wave function resides in the inner potential well for the $4d^9 4f\ ^3P, ^3D$ states but not for the $4d^9 4f\ ^1P_1$ state. Hence the Ba 4*d* giant resonance is best characterized as a shape resonance also. On passing to La and Ce, the maximum gets narrower and shifts towards the ionization threshold. The character of the excited electron wave function is expected to change from ϵf type to $(4,\epsilon)f$ type. Strong many-electron interactions lead to a rather complicated and fascinating situation.

The importance of the Ba, La, and Ce sequence is underscored by the numerous calculations based on different theoretical models. Total and partial cross sections have been obtained in the Hartree-Fock (HF) approximation, the random-phase approximation with exchange (RPAE), the (relativistic) time dependent local density approximation (RTDLDA), and the local-density-based random-phase approximation (LDRPA).[10,37–40,42–49] For a comparative discussion of the theoretical approaches the reader is referred to the recent articles by Crljen and Wendin.[50,51] An excellent compilation of recent review articles on giant resonances has been edited by Connerade *et al.*[52]

II. EXPERIMENT

For the photoabsorption measurements the atomic metals were maintained inside a resistance heated tubular furnace[53–55] mounted behind the exit slit of the HASYLAB toroidal grating monochromator (TGM).[56,57] The metals were contained in Ta tubes. The temperatures ranged from 1000 to 2200 K which according to vapor pressure data correspond to pressures between 0.1 and 0.5 mbar. The length of the vapor column was approximately 50 cm. Thin carbon windows together with a differential pumping stage separated the vapor region from the ultrahigh vacuum of the monochromator. He, Kr, or Xe buffer gas prevented the metal atoms from reaching the windows. The buffer gas also served to suppress higher-order background. The storage ring DORIS was used as a light source. The resolving power achieved with the TGM was $E/\Delta E = 800$. The spectra were recorded photoelectrically. Earlier experiments[3,12–16] were hampered with the difficulties encountered in determining reliable relative absorption cross

sections from photographically registered spectra. The density of the atoms in the vapor column has not been determined. Therefore only relative cross sections have been obtained.

For the photoelectron spectra the synchrotron radiation emitted by the electron storage ring BESSY was used. The radiation was monochromatized by a toroidal grating monochromator (TGM 2, $E/\Delta E = 330$).[58,59] The monochromatic photon beam (approximately 10^{11} photons/s) was focused on the interaction zone, where it crossed the atomic beam emanating from a furnace heated by indirect electron bombardment.[60] The density of the atoms in the interaction region is estimated to be $\simeq 10^{11}$ atoms/cm^3. The kinetic energy of electrons emerging from the interaction zone was determined by a cylindrical mirror analyzer (angular acceptance 0.8% of 4π, energy resolution $\Delta E = 0.74\%$ of the pass energy).[57] Only electrons emitted at angles close to the magic angle of 54°44′±1° relative to the principal axis of polarization of the incoming light were accepted by the analyzer. The relative partial cross sections were determined from a series of photoelectron spectra taken at different photon energies, from constant-ionic-state spectra (CIS), where the photon energy and the pass energy of the electron analyzer were scanned simultaneously and from constant-final-state spectra (CFS), where the photon energy was scanned while the analyzer energy was fixed. All spectra were normalized to the incoming photon flux and corrected for the energy-dependent bandpass of the electron spectrometer.

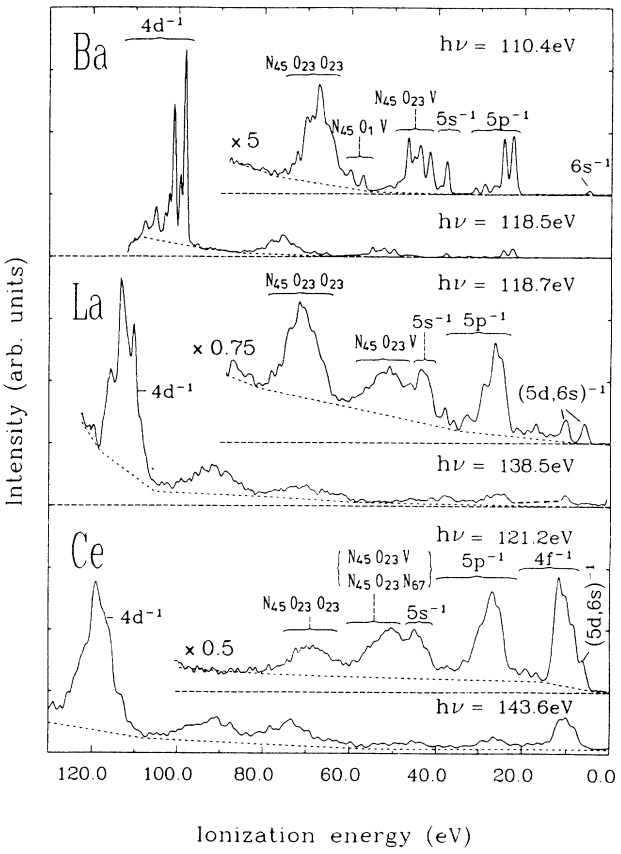

FIG. 1. Photoelectron spectra of atomic Ba, La, and Ce taken at photon energies in the range of the 4d giant resonance.

III. RESULTS AND DISCUSSION

A. Photoelectron spectra of atomic Ba, La, and Ce

The photoelectron spectra of atomic Ba, La, and Ce displayed in Fig. 1 give a survey of the photo and Auger lines emerging upon photoionization in the energy range of the 4d giant resonances. At the evaporation temperature of 800 K only the ground-state Ba, [Xe]$6s^2(^1S_0)$, is populated. Therefore all structures in the Ba spectrum are due to excitations out of the ground state. The well-resolved, spin-orbit split $5p^{-1}$ and $4d^{-1}$ photoelectron lines are easily detected. The prominent main lines are accompanied by a number of satellite lines which overlap the spin orbit doublets. There is a weak $6s^{-1}$ photoelectron line at the low-energy end of the spectrum. A host of Auger lines and the $5s^{-1}$ photoelectron lines occupy the center part of the spectrum. Ionization energies and assignment of the photoelectron lines are summarized in Table I. The assignment is based on optical data[27] and the $(Z+1)$ model. Our ionization energies agree well with other experimental data.[18,19]

Next we turn to the Ce spectrum shown in the bottom part of Fig. 1. Instead of sharp $5s^{-1}$, $5p^{-1}$, and $4d^{-1}$ photoelectron lines we see broad structured bands. Only to a small extent this can be attributed to the fact that at the evaporation temperature of 1800 K in addition to the Ce ground state [Xe]$4f5d6s^2(^1G_4)$ the Ce states [Xe]$4f5d6s^2(^3F_J,^3H_J,^3G_J)$ and [Xe]$4f5d^26s(^5H_J)$ are populated. The main effect rests with the multiplet splitting of the 4d, 5p, and 5s hole states caused by the interaction of the core hole with the collapsed 4f wave function. The multiplet lines overlap and give rise to the broad photoelectron and Auger maxima. The ionization energies and a tentative assignment are presented in Table II.

There is no 4f electron in the La configurations [Xe]$5d6s^2(^2D_J)$ and [Xe]$5d^26s(^4F_J)$ populated at the evaporation temperature of 1840 K. The 5d wave function has a small overlap with the core holes and therefore the multiplet splitting caused by the interaction of the core hole with the valence electrons should be small also. Based on this, the La photoelectron spectrum is expected to be similar to the Ba spectrum, e.g., show well resolved, spin-orbit split $4d^{-1}$ and $5p^{-1}$ photoelectron lines. However, the experimental spectrum of atomic La given in the center part of Fig. 1 looks much more like the Ce spectrum than the Ba spectrum. This experimental result can be explained by assuming that a collapsed 4f orbital becomes occupied in the final hold state. As for atomic Ce the 4f electron would cause a complicated multiplet structure of the La photoelectron and Auger lines.

In order to test this idea, we performed model calculations using the multiconfiguration Dirac-Fock (MCDF) code by Grant *et al.*[61]. In a first step we confirmed that

TABLE I. Ionization energies of atomic Ba, [Kr]$4d^{10}5s^25p^66s^2(^1S_0)$. The $6s^{-1}$ energy from optical data (Ref. 27) has been used for calibration. The uncertainties are approximately ±0.2 eV.

I (eV)	Ba II electron configuration	Core hole	I (eV)	Ba II electron configuration	Core hole
107.7	[Kr]$4d^9_{3/2}5s^25p^66s7s$	$4d^{-1}$	31.1	[Kr]$4d^{10}5s^25p^5_{1/2}6s7s$	$5p^{-1}$
106.0	[Kr]$4d^9_{3/2}5s^25p^66s6p$		29.1	[Kr]$4d^{10}5s^25p^5_{3/2}6s7s$	
105.3	[Kr]$4d^9_{5/2}5s^25p^66s7s$		29.1	[Kr]$4d^{10}5s^25p^5_{1/2}6s6p$	
103.1	[Kr]$4d^9_{5/2}5s^25p^66s6p$		26.2	[Kr]$4d^{10}5s^25p^5_{3/2}6s6p$	
102.0	[Kr]$4d^9_{3/2}5s^25p^66s4f$		26.2	[Kr]$4d^{10}5s^25p^5_{1/2}6s4f$	
101.0	[Kr]$4d^9_{3/2}5s^25p^66s^2$		24.7	[Kr]$4d^{10}5s^25p^5_{1/2}6s^2$	
99.5	[Kr]$4d^9_{5/2}5s^25p^66s4f$		22.7	[Kr]$4d^{10}5s^25p^5_{3/2}6s^2$	
98.4	[Kr]$4d^9_{5/2}5s^25p^66s^2$				
37.9	[Kr]$4d^{10}5s5p^66s^2$	$5s^{-1}$	5.2	[Kr]$4d^{10}5s^25p^66s$	$6s^{-1}$

the mixing between the configurations [Xe]$5d6s^2$ and [Xe]$4f6s6p$ for the La ground state is negligible. Increasing the nuclear charge by one unit, thus stimulating a core hole, lowers the energies of the states with $4f6s6p$ valence configuration with respect to the energies of the states with $5d6s^2$ valence configuration. Configuration mixing becomes important as is borne out by the results obtained for the ground state of this Ce^+-like ion. For simplification only those states of the above valence configurations most strongly admixed to the Ce^+-like ground state were taken into account in the subsequent calculation of the La $4d^{-1}$ multiplet. For comparison the Ba $4d^{-1}$ multiplet and the La $4d^{-1}5d6s^2$ multiplet, i.e., without configuration mixing, have also been calculated. The results are displayed in Fig. 2. In order to limit the numbers of lines, only the states with the highest J values ($J=4,5$) are given for the La $4d^{-1}$ multiplets.

The experimental results for atomic Ba and La and for La metal are included in Fig. 2. The Ba $4d^{-1}$ ionization energies and the spin-orbit splittings are well reproduced by the calculation [Fig. 2, (a) and (b)]. The calculated La $4d^{-1}5d6s^2$ multiplet fails to describe the experimental $4d^{-1}$ spectrum of atomic La, but is very close to the $4d^{-1}$ spectrum observed for La metal.[62] In agreement with the calculations, the spectrum of La metal shows two prominent lines separated by 2.8 eV. Extra-atomic screening is responsible for the atom-to-metal shift of the $4d$ binding energy by about 9 eV.[63,64] These findings are consistent with the well-known stabilization of the $5d$ level in the solid rare earths. Taking final-state configuration interaction into account, there is reasonable

TABLE II. Ionization energies of atomic La, [Xe]$5d6s^2$, [Xe]$5d^26s$ and Ce, [Xe]$4f5d6s^2$, [Xe]$4f5d^26s$. The $(5d,6s)^{-1}$ energy from optical data (Ref. 27) has been used for calibration. The uncertainties are approximately ±0.3 eV. Only the strongest line structures in the photoelectron spectra (Fig. 1) are listed here.

I (eV)	La II	I (eV)	Ce II	Core hole
115.7		122.0		$4d^{-1}$
113.2		119.3		
110.3		116.8		
44.4		45.6		$5s^{-1}$
42.4		43.9		
		42.2		
29.1		29.8		$5p^{-1}$
26.6		27.2		
24.8		25.5		
		19.3	[Xe]$(5d,6s)^27s$	$4f^{-1}$
		16.9	[Xe]$(5d,6s)^26p$	
		11.7	[Xe]$5d6s^2(^2D)$	
		10.0	[Xe]$5d^26s(^4F)$	
		8.7	[Xe]$4f5d6p$	
10.5	[Xe]$4f6p$		[Xe]$4f^26p$	$(5d,6s)^{-1}$
6.0	[Xe]$5d^2$	6.2	[Xe]$4f5d^2$	
	[Xe]$5d6s$		[Xe]$4f5d6s$	
	[Xe]$6s^2$		[Xe]$4f6s^2$	

agreement between the calculated [Fig. 2(f)] and the experimental atomic spectrum [Fig. 2(e)] with respect to the energies, the energy spread, and the fourfold structure.

In all photoelectron spectra of Fig. 1 a background can be observed. The background indicated by the broken line has been subtracted for the determination of the partial photoionization cross sections. Recent ion yield spectra[65,66] show that the $4d^{-1}(4,\epsilon)f$ excitations of Ba, La, and Ce mainly result in triply charged ions. Hence electrons emitted in the last steps of the multistep autoionization and Auger decay constitute part of the background. There is also $N_{4,5}$ double Auger emission buried in the background, since after background correction the $4d^{-1}$ intensity is systematically higher than the total intensity of the clearly perceptible $N_{45}O_{23}O_{23}$, $N_{45}O_1V$, $N_{45}O_{23}V$, and $N_{45}O_{23}N_{67}$ Auger lines. V stands here for "valence electron," e.g., O_{45} or P_1. For Ce also the $N_{45}N_{67}V$ Auger lines, which span a large energy range, contribute to the background.

B. Partial and total photoionization cross sections

1. Ba

The sum of all partial photoionization cross sections ($4d^{-1}$, $5s^{-1}$, $5p^{-1}$, and $6s^{-1}$) is given by the open circles in the upper part of Fig. 3. The partial cross sections are obtained from the main line and the satellite lines. The absorption spectrum has been normalized to the experimental total photoionization cross section at the low energy end and at the maximum at $h\nu=110$ eV. The normalization at the low-energy end eliminates the uncertainties due to the considerable errors involved in positioning the absorption spectra relative to the origin of the abscissa.[55] The absorption spectrum in Fig. 3 is in good agreement with a recent total ion yield spectrum.[65] This corroborates our normalization procedure. Our total photoionization cross section closely follows the absorption over the whole energy range. This demonstrates that the summation of the $4d^{-1}$, $5s^{-1}$, $5p^{-1}$, and $6s^{-1}$ partial cross sections includes all important channels contributing to the $4d^{-1}(4,\epsilon)f$ resonance. The experimental partial cross sections are presented in the center and the bottom part of Fig. 3. The $4d^{-1}$ partial cross section has been determined directly by the detection of the corresponding photoelectrons and indirectly by the detection of the N_{45} Auger electrons emitted upon the decay of the $4d^{-1}$ hole states. The indirect Auger cross section has been normalized to the direct photoelectron cross section in the photon energy range between 115 and 135 eV. The CFS spectrum represents the energy dependence of the $N_{4,5}$ Auger intensity.

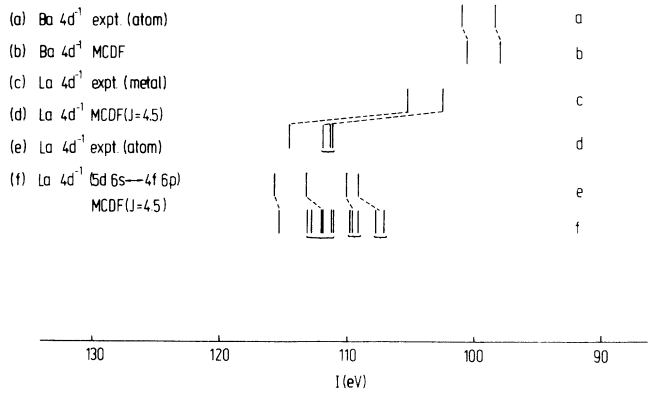

FIG. 2. Ba and La $4d^{-1}$ energy levels calculated by multiconfiguration Dirac-Fock method (Ref. 61) (b, d, and f). For comparison experimental results for atomic Ba and La and solid La (Ref. 62) are included (a, c, and e).

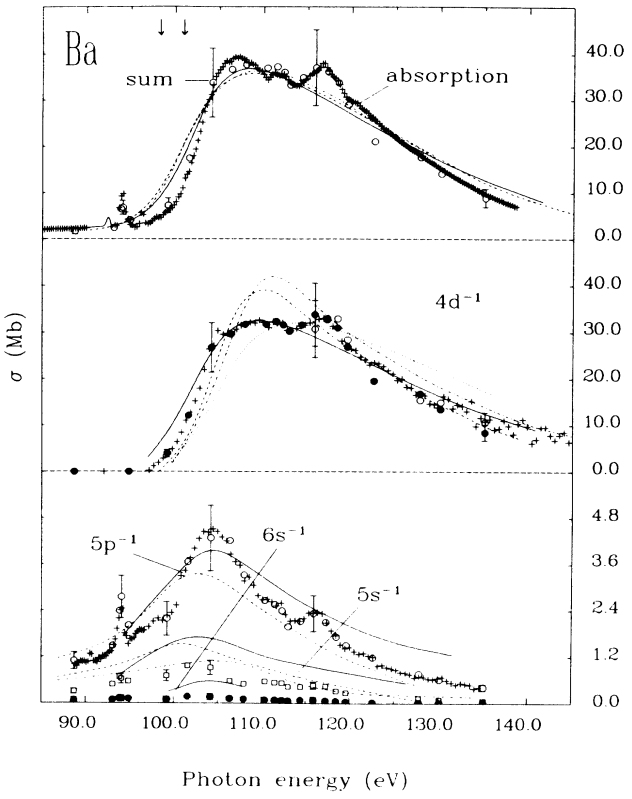

FIG. 3. Top: Experimental photoabsorption cross section (+) (Ref. 55) and theoretical photoionization cross sections (——) LDRPA (Ref. 49), and TDLDA [— — — (Ref. 48) and —·—·— (Ref. 70)] of atomic Ba. The sum of the partial cross sections is given by the open circles. The arrows mark the position of the $4d^{-1}$ ionization limits determined from the main photoelectron lines. Center: Ba $4d^{-1}$ partial cross section determined from the photoelectron lines (○) and the Auger lines (●) together with an Auger CFS spectrum (+). The results of LDRPA (——) (Ref. 49), HFR (· · · ·) (Ref. 38), and RPAE [— — — (Ref. 51) and —·—·— (Ref. 47)] calculations are included. Bottom: Experimental $5s^{-1}$ (□), $5p^{-1}$ [○, +(CIS)], and $6s^{-1}$ (●) partial cross sections of atomic Ba. The corresponding theoretical partial cross sections LDRPA (——) (Ref. 49), TDLDA (— — —) (Ref. 48), and RPAE (—·—·—·) (Ref. 45) are given for comparison.

Only relative cross sections could be determined in our experiments. The absolute cross sections in Fig. 3 refer to the theoretical spectra. In order to facilitate comparison the experimental spectra have been normalized to the theoretical spectra by multiplying by the factor which gives the best agreement for the total photoionization cross section and the $4d^{-1}$ partial photoionization cross section. In the range of overlap the results reported by Becker,[67] Bizau *et al.*,[68] and Bizau[69] agree with our data presented in Fig. 3.

The oscillator strength of the Ba $4d$ giant resonance is concentrated above the $4d^{-1}$ ionization limits determined from the $4d^{-1}$ photoelectron main lines. The arrows in the upper part of Fig. 3 indicate the energy positions of these ionization limits. The $4d^{-1}$ photoionization clearly dominates the resonance. Therefore the Ba $4d$ resonance can be interpreted as a $4d^{-1}\epsilon f$ atomic shape resonance similar to that of Xe and Cs (see Refs. 16, 21, and 31–40).

The partial $5s^{-1}$, $5p^{-1}$, and $6s^{-1}$ photoionization cross sections are resonantly enhanced in the range of the shape resonance. From Fig. 3 it is very clear that the $5s^{-1}$, $5p^{-1}$, and $6s^{-1}$ partial cross sections peak at photon energies well below the energy of the maximum of the total and partial $4d^{-1}$ photoionization cross section.

Except for the structures in the energy range between 105 and 120 eV LDRPA (Ref. 49) and TDLDA (Refs. 48 and 70) calculations describe the experimental total photoionization spectrum very well. The structures can be ascribed to two electron excitation processes, where in addition to the $4d$ electron an outer $6s$ or $5p$ electron is excited. Especially, processes involving the promotion of $5p$ electrons into the $5d$ shell are expected to substantially contribute to the peak located between 115 and 120 eV. Configuration interactions in the ground state, e.g., $5p^6 6s^2$-$5p^4 5d^2 6s^2$, and in the final state can be envisaged to be the main mechanism. A corresponding peak has been observed in the spectra of Ba^+ and Ba^{2+} (Ref. 71) and the Ba halides (Ref. 72). The experimental $4d^{-1}$ cross section is best reproduced by the LDRPA calculations.[49] The RPAE results[51,47] are closer to the experimental spectrum at threshold but markedly overshoot it in the maximum. The LDRPA (Ref. 49) and the TDLDA (Ref. 48) calculations are in reasonable agreement with the experimental $5p^{-1}$ partial cross section. In contrast to this, the calculations by far overestimate the $5s^{-1}$ and $6s^{-1}$ cross sections. Similar discrepancies have been found for Xe and Cs.[21,37,73,74] The calculations do not include two-electron channels that lead to correlation satellites in the experimental spectrum.[73,74] In analogy to Xe we expect final-state configuration interaction between the $5s5p^6 6s^2$ and $5s^2 5p^4 5d 6s^2$ configurations to transfer a considerable fraction of the $5s^{-1}$ electron oscillator strength to the two-electron satellites. Also ground-state configuration interaction between the $5s^2 5p^6 6s^2$ and $5s^2 5p^4 5d^2 6s^2$ is likely to contribute to the satellite intensity. In the experimental $5s^{-1}$ partial cross section part of this satellite intensity is missing because only the strongest satellites could be disentangled from the background and the Auger lines superimposed.

Figure 4 displays a series of photoelectron spectra taken at photon energies below the giant resonance (see Fig. 3). For the low-energy spectra, weak satellite lines are to be seen above the $5p^{-1}$ and the $5s^{-1}$ photoelectron lines. Tuning the photon energy to the multiline absorption band centered at 94 eV, the electron emission is strongly enhanced in the ionization energy range from 40 to 50 eV. The absorption band has been ascribed to $4d^{-1}4f(^3D_1)$ and $4d^{-1}6p$ excitations.[3,9,10,15,72,75,76] Resonant $N_{45}O_{23}O_{23}$ Auger decay of these excited states gives rise to the additional electron emission. The resonant Auger decay leads to similar $5p^4$ final state configurations as the $5s^{-1}$ satellite emission. In the spectrum taken at 99.2 eV, i.e., above the $4d^{-1}$ ionization limit, the normal $N_{45}O_{23}O_{23}$ Auger emission emerges between 50 and 60 eV on the ionization energy scale. This corresponds to kinetic energies of the Auger electrons between 40 and 50 eV. Due to the screening by the bound excited electron, the kinetic energy of the electrons emitted upon the resonant Auger decay is approximately 5 eV higher. Tuning the photon energy through the $(4d^{-1}4f(^3D_1), 4d^{-1}6p)$ resonance causes a dramatic change of the $5p_{3/2}^{-1}$ to $5p_{1/2}^{-1}$ branching ratio. Similar effects have been observed and discussed for atomic Xe and Cs.[21,77–79] The enhancement of the satellite intensity and the change of the $5p_{3/2}^{-1}$ to $5p_{1/2}^{-1}$ branching ratio has also been observed by Bizau.[69]

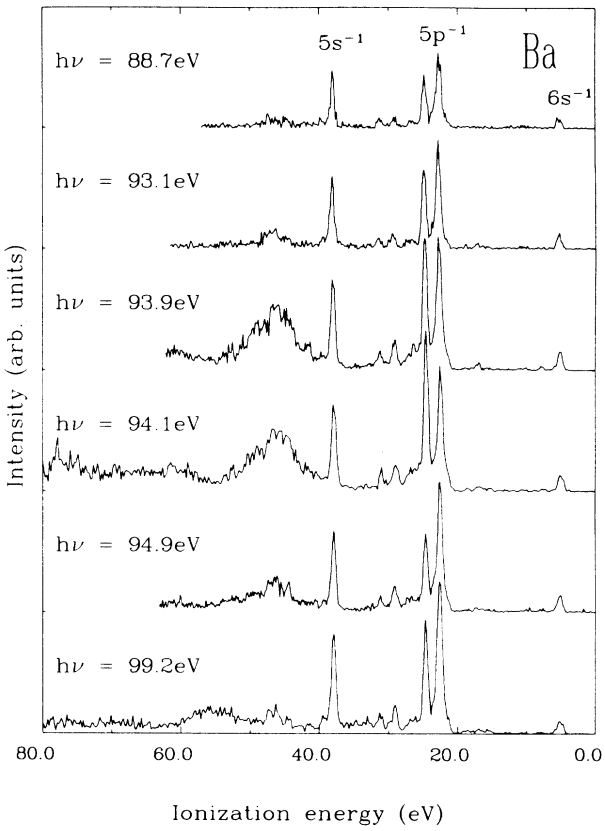

FIG. 4. Photoelectron spectra of atomic Ba taken at photon energies in the range of the fine structure below the giant resonance.

2. La

For atomic La, the absorption spectrum,[54] the $4d^{-1}$, $5s^{-1}$, $5p^{-1}$, and $(5d,6s)^{-1}$ partial cross sections and the sum of these partial cross sections are displayed in Fig. 5. The normalization between the experimental absorption spectrum, the photoionization data, and the theoretical cross sections has been performed in the same way as described for atomic Ba. The arrows in the upper part of Fig. 5 mark the position of the ionization limits derived from the main photoelectron lines. The total photoionization cross section and the $4d^{-1}$ partial cross section peak above these limits. Compared to Ba the maxima have moved closer to the limits. The $4d^{-1}$ partial cross section dominates the giant resonance. As for Ba the $4d^{-1}$ cross section has been determined from the strength of the $4d^{-1}$ photoelectron lines and the strength of the $N_{45}O_{23}O_{23}$ Auger lines. The photon energy dependence of the $N_{45}O_{23}O_{23}$ intensity is given by the CFS spectrum. The Auger spectra have been normalized to the photoelectron data in the region of overlap. The $5p^{-1}$, $5s^{-1}$, and $(5d,6s)^{-1}$ partial cross sections are resonantly enhanced in the range of the giant resonance. These outer-shell partial cross sections peak at photon energies below the peak energy of the total and $4d^{-1}$ partial cross section. The cross sections indicate that the interchannel coupling is stronger than in the case of Ba. The close similarity to the Ba spectra is a clear evidence that the character of the resonance has been conserved when going from Ba to La. The total photoionization cross section and the $4d^{-1}$ partial cross section are very well described by the LDRPA calculations.[49] The results of the pioneering HS calculations[10] for the total cross section and those of RTDLDA (Ref. 80) for the $4d^{-1}$ partial cross section differ considerably from the experimental curves. In contrast to the case of a Ba both calculations[49,80] underestimate the $5p^{-1}$, $5s^{-1}$, and $(5d,6s)^{-1}$ partial cross sections, respectively. Peak position and shape of the experimental spectra are much closer to the LDRPA spectra[49] than to the RTDLDA (Ref. 80) spectra.

The spectra in Fig. 5 do not display prominent structures which could be ascribed in two electron excitation processes. Still there is a clue that two electron excitations contribute to the absorption. Figure 6 shows the partial cross sections for the two low-energy photoelectron lines (see Fig. 1) tentatively assigned to La II final states $[Xe](5d6s)^2$ and $[Xe]4f6p$. There is a coupling to the giant resonances for both lines but their cross sections peak at different energies. In order to determine the resonance energies, the experimental points have been approximated by a superposition of Fano-type profiles,[30,81–87]

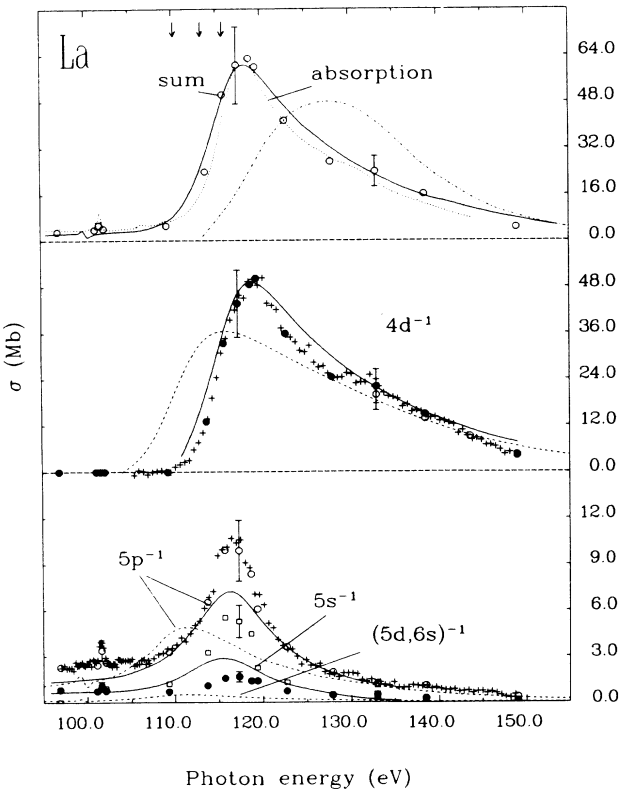

FIG. 5. Top: Experimental photoabsorption cross section (· · · ·) and theoretical photoionization cross sections LDRPA (——) (Ref. 49), HS (—·—·—·) (Ref. 10) of atomic La in comparison to the sum of the partial photoionization cross sections (○). The arrows mark the position of the $4d^{-1}$ ionization thresholds determined from the main photoelectron lines. Center: La $4d^{-1}$ partial cross section determined from the photoelectron lines (○) and the Auger lines (●) together with an Auger CFS spectrum (+). The results of LDRPA (——) (Ref. 49) and RTDLDA (— — —) (Ref. 80) calculations are included. Bottom: Experimental $5s^{-1}$ (□), $5p^{-1}$ [○+(CIS)], and $(5d6s)^{-1}$ (●) partial cross sections of atomic La. The corresponding theoretical cross sections LDRPA (——) (Ref. 49) and RTDLDA (— — —) (Ref. 80) are given for comparison.

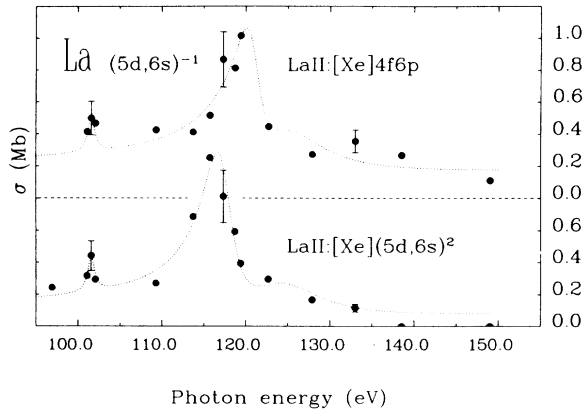

FIG. 6. Partial $(5d6s)^{-1}$ photoionization cross sections of atomic La. Bottom: main photoelectron line La II, $[Xe](5d6s)^2$. Top: satellite line La II, $[Xe]4f6p$. The dotted lines represent an approximation to the data points by a superposition of Fano-type profiles.

$$\sigma_P(h\nu)=\sigma_{b,P}+\sum_n \sigma_{a,P,n}\frac{\left[q_{P,n}+\frac{h\nu-h\nu_n}{\Gamma_n/2}\right]^2}{1+\left[\frac{h\nu-h\nu_n}{\Gamma_n/2}\right]^2}. \quad (1)$$

P denotes the photoionization channel. The sum extends over all resonances n characterized by a resonance energy $h\nu_n$ and a halfwidth Γ_n. The asymmetry parameters $q_{P,n}$ and the interacting cross section $\sigma_{a,P,n}$ depend on the photoionization channel and the resonance. The noninteracting background is given by $\sigma_{b,P}$. Note that in the case of many interacting continua and resonances this parametrization represents a considerable simplification and therefore can only be considered as an empirical method to describe the spectra. The curves obtained by the fitting procedure are included in Fig. 6. The parameters are listed in Table III. Here we are mostly interested in the fact that for the La II channel $[Xe](5d6s)^2$ the dominant resonance lies at 117.3 eV, i.e., close to the peak position of the total and $4d^{-1}$, $5p^{-1}$, and $5s^{-1}$ partial cross sections, whereas for the La II channel $[Xe]4f6p$ the strongest resonance is located at 121 eV. A possible explanation could be that multiple electron excitations involving the transfer of valence electrons into the $4f$ orbital are responsible for the resonance. Both spectra in Fig. 5 indicate the existence of another resonance at 124 eV. The existence of this resonance is corroborated by the weak shoulder at $\cong$130 eV in the absorption spectrum and the $4d^{-1}$ partial cross section. This resonance is a further candidate for multielectron excitation.

3. Ce

The absorption spectrum of atomic Ce (Ref. 54) and the sum of the $4d^{-1}$, $5s^{-1}$, $5p^{-1}$, $4f^{-1}$, and $(5d,6s)^{-1}$ partial cross sections are given in the upper part of Fig. 7. As for Ba and La the absorption has been normalized to the sum of the partial cross sections. The $4d^{-1}$ spectra have been determined in the same way as for Ba and La. The relative experimental spectra have been put on an absolute scale by normalizing the experimental $4d^{-1}$ partial cross section to the $4d^{-1}$ cross section calculated within the RTDLDA.[80] In order to correct for discrepancies between theory and experiment in respect to energy positions and relative strength of the partial cross sections we (i) shifted all theoretical cross sections except the $4f^{-1}$ partial cross section by 4.7 eV towards higher energies, (ii) multiplied the theoretical $4f^{-1}$, $5s^{-1}$, $5p^{-1}$, and $(5d,6s)^{-1}$ partial cross sections by a factor of 2.

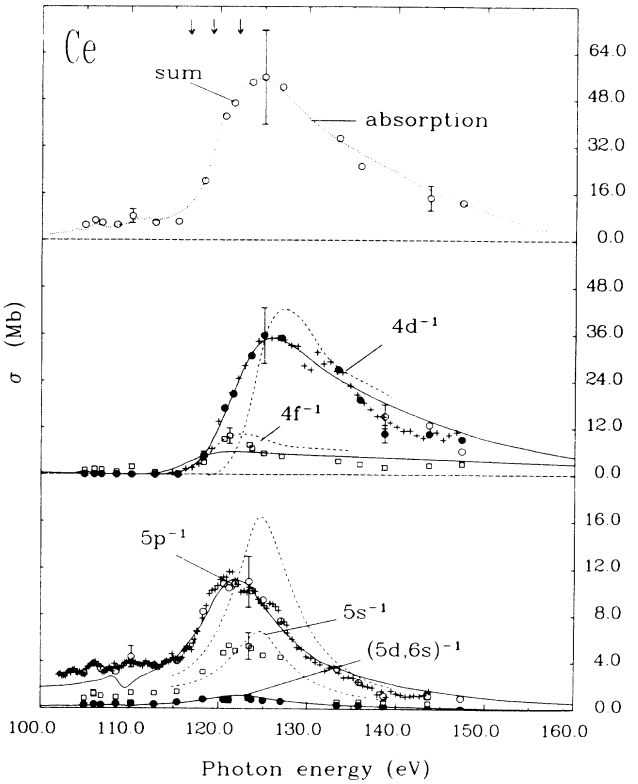

FIG. 7. Top: Experimental photoabsorption cross section (· · · ·) and the sum of the partial photoionization cross sections (○) of atomic Ce. The arrows mark the position of the $4d^{-1}$ ionization limits determined from the main photoelectron lines. Center: Ce $4d^{-1}$ partial cross section determined from the photoelectron lines (○) and the Auger lines (●) together with an Auger CFS spectrum (+) and $4f^{-1}$ partial cross section (□). The results of RTDLDA (——) (Ref. 80) and TDLDA (— — —) (Ref. 48) calculation are included. Bottom: Experimental $5s^{-1}$ (□), $5p^{-1}$ [○, +(CIS)], and $(5d6s)^{-1}$ (●) partial cross sections of atomic Ce. The corresponding theoretical cross sections RTDLDA (——) (Ref. 80) and TDLDA (— — —) (Ref. 48) are given for comparison. Except the $4d^{-1}$ partial cross section, all theoretical cross sections have been multiplied by a factor of 2 and with the exception of the $4f^{-1}$ partial cross section all have been shifted towards higher photon energies by 4.7 eV.

These operations result in good agreement between the RTDLDA spectra[80] and the experimental spectra. The TDLDA calculations[48] describe the $4f^{-1}$ and $5s^{-1}$ par-

TABLE III. Parameters determined by approximating the La spectra in Fig. 6 by a superposition of Fano profiles according to Eq. (1) with $\sigma_{b,P}=0$.

			La II $[Xe](5d,6s)^2$		La II $[Xe]4f6p$	
n	$h\nu_n$ (eV)	Γ_n (eV)	q	$\sigma_a q^2$ (Mb)	q	$\sigma_a q^2$ (Mb)
1	101.6	1.0	∞	0.22	∞	0.21
2	117.3	4.4	−2.9	0.87		
3	121.0	3.6			−1.7	0.57
4	124	12	∞	0.27	∞	0.42

tial cross sections reasonably well, whereas for the $4d^{-1}$ and $5p^{-1}$ cross sections theory still deviates from the experimental results. Along the series Ba, La, and Ce the outer shell partial cross sections systematically increase. For La and Ce the calculations underestimate the coupling between the $4d^{-1}(4,\epsilon)f$ excitations and the outer-shell ionizations. From Fig. 7 one can deduce an approximate value of 4 for the ratio between the $4d^{-1}$ cross section and the $4f^{-1}$ cross section. The TDLDA calculations[48] predicted a value of 8 for the same ratio. Earlier measurements[20] indicated an even greater discrepancy between theory and experiment, but this was due to a too low $4d^{-1}$ cross section. The outer-shell ionization is mainly concentrated close to the 4d ionization thresholds whereas the $4d^{-1}$ ionization prevails towards higher energies. Total ionization and $4d^{-1}$ cross section display the profile characteristics for shape resonances. The $5p^{-1}$ CIS spectrum shows structure not only below the resonance, but also on the high-energy slope. A fit according to Eq. (1) yields resonance positions at 120.1, 122.3, 123.8, 126.5, and 130 eV. Excited state multiplet splitting[9,12] and multiple electron excitations are possible explanations. Close to the ionization thresholds we expect $4d^{10}4f \rightarrow 4d^{9}4f^{2}$-type transitions to contribute. This expectation is based on the strong resonant enhancement of the $4f^{-1}$ photoelectron lines in this energy range. The partial cross sections of the $4f^{-1}$ photoelectron lines listed in Table II are given in Fig. 8. The uppermost curve represents the cross section of the two lines assigned to Ce II final states $[Xe](5d,6s)^2 6p,7s$. The bottom curve has been obtained by summing all lines ascribed to Ce II final states $[Xe]4f(5d,6s)^2$ (see Table II). The data have been approximated by a superposition of Fano-type profiles [Eq. (1)]. The parameters are summarized in Table IV. The low-energy resonances ($h\nu = 106$ eV; 110.1 eV) coincide with strong absorption lines of atomic Ce.[12,54] The resonances at 120.1 and 122.3 eV have their counterpart in a marked shoulder in the absorption spectrum, which spans the energy range from 120 to 124 eV. The latter resonances preferentially decay into the $4f \rightarrow \epsilon l$ continuum. The asymmetric profiles are readily explained by the interference of $4d \rightarrow 4f$-type excitations with the $4f \rightarrow \epsilon l$ ionization continuum. Thus our photoelectron spectra corroborate the

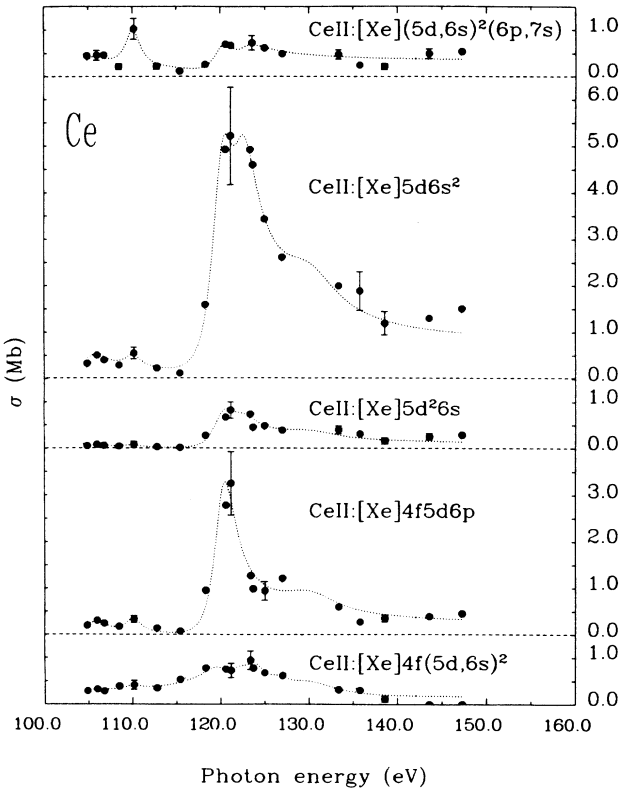

FIG. 8. Ce $(5d6s)^{-1}$ partial photoionization cross section (bottom) and different $4f^{-1}$ partial cross sections. The dotted lines represent the approximation of the data points by a superposition of Fano-type profiles.

assignment of these resonances to $4d^{10}4f \rightarrow 4d^{9}4f^{2}$ transitions.[9,12] The asymmetric resonance profile of the line assigned to the Ce II final state $[Xe]4f5d6p$ clearly favors an interpretation in terms of an $4d \rightarrow 4f$ excitation, autoionizing into the $4f \rightarrow \epsilon l$ continuum. This casts doubts on our tentative assignment, which is based on the tabulated atomic energy levels.[27] If we do not want to discard the assignment, we could invoke initial or final state

TABLE IV. Parameters determined by approximating the Ce spectra in Fig. 8 by a superposition of Fano profiles according to Eq. (1) with $\sigma_{b,P}=0$.

			Ce II states									
			$[Xe]4f(5d,6s)^2$		$[Xe]4f5d6p$		$[Xe]5d^26s$		$[Xe]5d6s^2$		$[Xe](5d,6s)^2(6p,7s)$	
n	$h\nu_n$ (eV)	Γ_n (eV)	q	$\sigma_a q^2$ (Mb)	q	$\sigma_a q^2$ (Mb)	q	$\sigma_a q^2$ (Mb)	q	$\sigma_a q^2$ (Mb)	q	$\sigma_a q^2$ (Mb)
1	106.0	2.0	∞	0.03	∞	0.21	∞	0.03	∞	0.21	∞	0.18
2	110.1	2.0	∞	0.09	∞	0.30	∞	0.05	∞	0.24	∞	0.78
3	120.1	3.3	−1.5	0.27	3.8	3.03	3.6	0.72	5.0	4.65	2.8	0.60
4	122.3	3.3	−2.2	0.36			2.4	0.24	2.2	2.31	0.7	0.12
5	123.8	3.3	∞	0.66								
6	126.5	3.3	∞	0.21								
7	130	8	∞	0.33	∞	0.45	∞	0.15	∞	0.90		

configuration interactions which result in a rearrangement of the valence electrons and an occupied $4f$ orbital in the ionic final state. Similar processes have been discussed above for atomic La. An essential result of the photoelectron spectroscopy is the change of the character of the excitations contributing to the giant resonance from $4d$-$4f$ type of threshold to $4d$-ϵf ionization at higher photon energies. It is interesting to note that the partial cross sections for solid Ce (Ref. 6) are very similar to those of atomic Ce.

ACKNOWLEDGMENTS

The authors wish to thank the BESSY and the HASYLAB staff for continuous assistance and Gary Doolen (Los Alamos National Laboratory) and Andrew Zangwill (Georgia Institute of Technology) for providing us with their unpublished RTDLDA results. The financial support by the Bundesministerium für Forschung und Technologie der Bundesrepublik Deutschland is gratefully acknowledged.

[1]T. M. Zimkina, V. A. Fomichev, S. A. Gribovskii, and I. I. Zhukova, Fiz. Tverd. Tela **9**, 1447 (1967); **9**, 1490 (1967) [Sov. Phys.–Solid State **9**, 1128 (1967); **9**, 1163 (1967)].

[2]R. Haensel, P. Rabe, and B. Sonntag, Solid State Commun. **8**, 1845 (1970).

[3]P. Rabe, K. Radler, and H.-W. Wolff, in *VUV Radiation Physics,* edited by E. E. Koch *et al.* (Vieweg-Pergamon, Braunschweig, 1974), p. 247.

[4]T. M. Zimkina, A. S. Shulakov, V. A. Fomichev, A. P. Braiko, and A. P. Stepanev, in *X-Ray and Inner-Shell Processes in Atoms, Molecules and Solids,* edited by A. Meisel and J. Finster (Karl-Marx-Universität, Leipzig, 1984), p. 263.

[5]M. H. Hecht and I. Lindau, Phys. Rev. Lett. **47**, 821 (1981).

[6]F. Gerken, J. Barth, and C. Kunz, in *X-Ray and Atomic Inner-Shell Physics, (University of Oregon, Eugene, Oregon),* Proceedings of the International Conference on X-Ray and Atomic Inner-Shell Physics, 1982, AIP Conf. Proc. No. 94, edited by B. Crasemann (AIP, New York, 1982), p. 602.

[7]J. C. Rivière, F. P. Netzer, G. Rosina, G. Strasser, and J. A. D. Matthews, J. Electron Spectrosc. Relat. Phenom. **36**, 331 (1985).

[8]J. L. Dehmer, A. F. Starace, U. Fano, J. Sugar, and J. W. Cooper, Phys. Rev. Lett. **26**, 1521 (1971).

[9]J. Sugar, Phys. Rev. B **5**, 1785 (1972).

[10]J. L. Dehmer and A. F. Starace, Phys. Rev. B **5**, 1792 (1972).

[11]M. W. D. Mansfield and J. P. Connerade, Proc. R. Soc. London, Ser. A **352**, 125 (1976).

[12]H.-W. Wolff, R. Bruhn, and B. Sonntag, Phys. Lett. **59A**, 67 (1976).

[13]E.-R. Radtke, J. Phys. B **12**, L71 (1979); **12**, L77 (1979).

[14]J. P. Connerade and M. W. D. Mansfield, Proc. R. Soc. London, Ser. A **341**, 267 (1974).

[15]D. L. Ederer, T. B. Lucatorto, R. P. Madden, and J. Sugar, J. Phys. B **8**, L21 (1975).

[16]T. B. Lucatorto, T. J. McIlrath, W. T. Hill, and C. W. Clark, in *X-Ray and Atomic Inner-Shell Physics (University of Oregon, Eugene, Oregon),* Proceedings of the International Conference on X-Ray and Atomic Inner-Shell Physics, 1982, AIP Conf. Proc. No. 94, edited by B. Crasemann (AIP, New York, 1982), p. 584.

[17]B. Sonntag and F. Wuilleumier, Nucl. Instrum. and Methods **208**, 735 (1983).

[18]F. J. Wuilleumier, J. M. Bizau, G. Wendin, and P. Dhez, in Book of Abstracts, International Conference on X-ray and Atomic Inner-Shell Physics, Oregon, 1982 (unpublished) p. 153.

[19]U. Becker, R. Hölzel, H. G. Kerkhoff, B. Langer, D. Szostak, and R. Wehlitz, *Abstracts of Contributed Papers, Fourteenth International Conference on the Physics of Electronic and Atomic Collisions, Palo Alto, 1985,* edited by M. J. Coggiola, D. L. Huestis, and R. P. Saxon (North-Holland, Amsterdam, 1986), p. 12.

[20]M. Meyer, T. Prescher, E. v. Raven, M. Richter, E. Schmidt, B. Sonntag, and H.-E. Wetzel, Z. Phys. D **2**, 347 (1986).

[21]T. Prescher, M. Richter, E. Schmidt, B. Sonntag, and H.-E. Wetzel, J. Phys. B **19**, 1645 (1986).

[22]U. Becker, H. G. Kerkhoff, D. W. Lindle, P. H. Kobrin, T. A. Ferrett, P. A. Heimann, C. M. Truesdale, and D. A. Shirley, Phys. Rev. A **34**, 2858 (1986).

[23]D. C. Griffin, K. L. Andrew, and R. D. Cowan, Phys. Rev. **177**, 62 (1969).

[24]J. P. Connerade, Contemp. Phys. **19**, 415 (1978).

[25]K. T. Cheng and C. Froese Fischer, Phys. Rev. A **28**, 2811 (1983).

[26]K. T. Cheng and W. R. Johnson, Phys. Rev. A **28**, 2820 (1983).

[27]W. C. Martin, R. Zalubas, and L. Hagan, *Atomic Energy Levels-The Rare-Earth Elements,* Natl. Bur. Stand. Ref. Data Ser., Natl. Bur. Stand. (U.S.) Circ. No. 60 (U. S. GPO, Washington, D. C., 1978).

[28]R. C. Karnatak, J. M. Esteva, and J. P. Connerade, J. Phys. B **14**, 4747 (1981).

[29]B. Sonntag, T. Nagata, Y. Sato, Y. Satow, A. Yagishita, and M. Yanigahara, J. Phys. B **17**, L55 (1984).

[30]F. Combet Farnoux, Phys. Rev. A **25**, 287 (1982).

[31]D. L. Ederer, Phys. Rev. Lett. **13**, 760 (1964).

[32]R. Haensel, G. Keitel, P. Schreiber, and C. Kunz, Phys. Rev. **188**, 1375 (1969).

[33]U. Fano and J. W. Cooper, Rev. Mod. Phys. **40**, 441 (1968).

[34]J. A. R. Samson, in *Handbuch der Physik,* edited by W. Mehlhorn (Springer-Verlag, Berlin, 1982), Vol. 31, p. 123.

[35]A. F. Starace, in *Corpuscles and Radiation in Matter I,* Vol. 31 of *Handbüch der Physik,* edited by W. Mehlhorn (Springer-Verlag, Berlin, 1982), p. 1.

[36]D. M. P. Holland, K. Codling, J. P. West, and G. V. Marr, J. Phys. B **12**, 2465 (1979).

[37]M. Ya. Amusia, in *Atomic Physics,* edited by I. Lindgren, A. Rosén, and S. Svanberg (Plenum, New York, 1983), Vol. 8, p. 287.

[38]H. P. Kelly, in *Atomic Physics,* edited by I. Lindgren, A. Rosén, and S. Svanberg (Plenum, New York, 1983), Vol. 8, p. 305.

[39]H. P. Kelly, Phys. Scr. **T17**, 109 (1987).

[40]A. Zangwill, in *Atomic Physics,* edited by I. Lindgren, A. Rosén, and S. Svanberg (Plenum, New York, 1983), Vol. 8, p. 339.

[41]G. Wendin and A. F. Starace, J. Phys. B **11**, 4119 (1978).
[42]H. P. Kelly, S. L. Carter, and B. E. Norum, Phys. Rev. A **25**, 2052 (1982).
[43]G. Wendin, Phys. Lett. **46A**, 119 (1973).
[44]A. W. Fliflet, R. L. Chase, and H. P. Kelly, J. Phys. B **7**, L443 (1974).
[45]M. Ya. Amusia, in *VUV Radiation Physics,* edited by E. E. Koch *et al.* (Vieweg-Pergamon, Braunschweig, 1974), p. 205.
[46]G. Wendin, in *VUV Radiation Physics,* edited by E. E. Koch *et al.* (Vieweg-Pergamon, Brauschweig, 1974), p. 225.
[47]M. Ya. Amusia, V. K. Ivanov, and L. V. Chernysheva, Phys. Lett. **59A**, 191 (1976).
[48]A. Zangwill and P. Soven, Phys. Rev. Lett. **45**, 204 (1980).
[49]G. Wendin, in *New Trends in Atomic Physics,* Les Houches Summer School 1982, edited by G. Grynberg and R. Stora (Elsevier, Amsterdam, 1984), p. 555.
[50]Z. Crljen and G. Wendin, Phys. Scr. **32**, 359 (1985).
[51]Z. Crljen and G. Wendin, Phys. Rev. A **35**, 1555 (1987); **35**, 1571 (1987).
[52]*Giant Resonances in Atoms, Molecules, and Solids,* edited by J. P. Connerade, J. M. Esteva, and R. C. Karnatak (Plenum, New York, 1987).
[53]R. Bruhn, Thesis, Universität Hamburg, Hamburg, Germany, 1979; DESY Internal Report No. F41-79-08 (unpublished).
[54]M. Pahler, Diplomarbeit, Universität Hamburg, Hamburg, Germany, 1987.
[55]D. Handschuh, Diplomarbeit, Universität Hamburg, Hamburg, Germany, 1987.
[56]R. Bruhn, E. Schmidt, H. Schröder, B. Sonntag, A. Thevenon, G. Passereau, and J. Flamand, Nucl. Instrum. Methods **208**, 771 (1983).
[57]H. Schröder, Thesis, Universität Hamburg, 1982; DESY Internal Report No. F41-83-05, 1983 (unpublished).
[58]W. Braun, G. Jäkisch, A. Baalman, and W. Radlitz, BESSY Annual Report, 1983 (unpublished).
[59]W. Braun, G. Jäkisch, H. Kuhlenbeck, M. Richter, M. Meyer, and T. Prescher, in BESSY Annual Report, 1986 (unpublished).
[60]T. Prescher, M. Richter, B. Sonntag, and H. E. Wetzel, Nucl. Instrum. Methods A **254**, 627 (1987).
[61]I. P. Grant, B. J. McKenzie, P. H. Norrington, D. F. Mayers, and N. C. Pyper, Comput. Phys. Commun. **21**, 207 (1980).
[62]S. P. Kowalczyk, N. Edelstein, F. R. McFeely, L. Ley, and D. A. Shirley, Chem. Phys. Lett. **29**, 491 (1974).
[63]See, e.g., J. F. Herbst, J. Less-Common Metals **93**, 227 (1983).
[64]M. Richter, T. Prescher, M. Meyer, E. v. Raven, B. Sonntag, H.-E. Wetzel, and S. Aksela, Phys. Rev. B **38**, 1763 (1988).
[65]A. Yaghishita *et al.* (unpublished).
[66]Ch. Dziouk, W. Fiedler, M. V. Lucke, and P. Zimmermann, Phys. Rev. Lett. **62**, 878 (1989).
[67]U. Becker, in *Giant Resonances in Atoms, Molecules and Solids,* edited by J. P. Connerade, J. M. Esteva, and R. C. Karnatak (Plenum, New York, 1987), p. 473.
[68]J. M. Bizau, D. Cubaynes, P. Gerard, F. J. Wuilleumier, and J. L. Picque, in *X-Ray and Inner-Shell Processes,* edited by P. Lagarde, F. J. Wuilleumier, and J.-P. Briand (les éditions de Physique, Les Ulis Cedex, 1987), Vol. I, C9-491.
[69]J.-M. Bizau, Thesis, Université de Paris Sud, 1987.
[70]K. Nuroh, E. Zaremba, and M. J. Stott, Phys. Rev. Lett. **49**, 862 (1982).
[71]C. W. Clark and T. B. Lucatorto, in *Giant Resonances in Atoms, Molecules and Solids,* edited by J. P. Connerade, J. M. Esteva, and R. C. Karnatak (Plenum, New York, 1987), p. 137.
[72]P. Rabe, Thesis, Universität Hamburg, 1974; DESY Internal Report No. F41-74/2, 1974 (unpublished).
[73]M. Ya. Amusia, in *International Conference on X-Ray and Inner-Shell Processes in Atoms, Molecules and Solids,* edited by A. Meisel and J. Finster (Karl-Marx-Universität, Leipzig, 1984), p. 33.
[74]A. Fahlman, M. O. Krause, T. A. Carlson, and A. Svensson, Phys. Rev. A **30**, 812 (1984).
[75]D. L. Ederer, T. B. Lucatorto, E. B. Saloman, R. P. Madden, M. Manalis, and J. Sugar, in *Electron and Photon Interactions with Atoms,* edited by H. Kleinpoppen and M. R. C. McDowell (Plenum, New York, 1976), p. 69.
[76]H.-W. Wolff, Thesis, Universität Hamburg, Hamburg, Germany, 1980; DESY Internal Report No. F41-80-07, 1980 (unpublished).
[77]K. N. Huang, W. R. Johnson, and K. T. Cheng, At. Data Nucl. Data Tables **26**, 33 (1981).
[78]F. A. Parpia and W. R. Johnson, J. Phys. B **17**, 531 (1984).
[79]U. Becker, T. Prescher, E. Schmidt, B. Sonntag, and H.-E. Wetzel, Phys. Rev. A **33**, 3891 (1986).
[80]A. Zangwill and G. Doolen (unpublished).
[81]U. Fano, Phys. Rev. **124**, 1866 (1961).
[82]U. Fano and J. W. Cooper, Phys. Rev. **137**, A1364 (1965).
[83]B. W. Shore, Phys. Rev. **171**, 43 (1968).
[84]F. H. Mies, Phys. Rev. **175**, 164 (1968).
[85]P. C. Kemeny, J. A. R. Samson, and A. F. Starace, J. Phys. B **10**, L201 (1977).
[86]L. C. Davis and L. A. Feldkamp, Phys. Rev. B **23**, 6239 (1981).
[87]M. Meyer, T. Prescher, E. v. Raven, M. Richter, E. Schmidt, B. Sonntag, and H.-E. Wetzel, in *Giant Resonances in Atoms, Molecules and Solids,* edited by J. P. Connerade, J. M. Esteva, and R. C. Karnatak (Plenum, New York, 1987), p. 251.